



an ASME
publication

Copyright © 1979 by ASME

The Society shall not be responsible for statements or opinions advanced in papers or in discussion at meetings of the Society or of its Divisions or Sections, or printed in its publications. *Discussion is printed only if the paper is published in an ASME journal or Proceedings.*

Released for general publication upon presentation.

Full credit should be given to ASME, the Technical Division, and the author(s).

\$3.00 PER COPY

\$1.50 PER COPY ASME MEMBERS

ROCKETDYNE LIBRARY

Performance Estimation of Partial Admission Turbines

KOJI KOREMATSU

Kogakuin University,
Shinjuku-ku, Tokyo, Japan

NAOMICHI HIRAYAMA

Tokyo Metropolitan University,
Setagaya-ku, Tokyo, Japan

The new relationships of partial admission losses which account for influence of all major geometric parameters of concern to the turbine designer are presented, based on fluid dynamic analysis of the losses. The performance maps are presented showing the trends in efficiencies that are attainable in turbine designed over a wide range of loading, axial velocity/blade speed ratio, Reynolds number, and aspect ratio. Finally, the question of partial admission versus low aspect ratio is discussed.

Contributed by the Gas Turbine Division of The American Society of Mechanical Engineers for presentation at the Gas Turbine Conference & Exhibit & Solar Energy Conference, San Diego, Calif., March 12-15, 1979. Manuscript received at ASME Headquarters December 18, 1978.

Copies will be available until December 1, 1979.

Performance Estimation of Partial Admission Turbines

KOJI KOREMATSU

NAOMICHI HIRAYAMA

ABSTRACT

The new relationships of partial admission losses which account for influence of all major geometric parameters of concern to the turbine designer are presented, based on fluid dynamic analysis of the losses. The performance maps are presented showing the trends in efficiencies that are attainable in turbine designed over a wide range of loading, axial velocity/blade speed ratio Reynolds number and aspect ratio. Finally, the question of partial admission versus low aspect ratio is discussed.

NOMENCLATURE

$A := \frac{\zeta}{2} \sin^2 \beta_2 - 1/2 \left\{ \frac{\sin \beta_3}{\sin \alpha_2} (\cos \alpha_2 - \frac{\sin \alpha_2}{\tan \beta_2}) - \cos \alpha_2 / (\cos \alpha_2 - \frac{\sin \alpha_2}{\tan \beta_2}) \right\}$
 $A_1 := -\frac{1}{2} + \zeta \frac{\sin^2 \beta_2}{2} - \frac{C_1^2}{2u^2}$
 $B := \cos \alpha_2 \sin \beta_3 / \sin \alpha_2 - \zeta \sin \beta_2 \sin(\beta_2 - \alpha_2) \sin \beta_3 / \sin \alpha_2$
 $C := \frac{1}{2} \left\{ 1 + \zeta \sin^2(\beta_2 - \alpha_2) \left(\frac{\sin \beta_3}{\sin \alpha_2} \right)^2 \right\}$
 C : pumping loss coefficient
 C_0 : pumping loss coefficient without plates
 c : chord length
 c_{xp} : axial velocity under partial admission
 c_x : axial velocity under full admission or at steady state
 $D := B^2 - 4AC$
 $D_1 := B^2 - 4A_1C$
 D_m : mean diameter
 D_0 : outer diameter of rotor disc
 D : pitch circle diameter of rotor disc
 $E_m := (B - \sqrt{D}) / (B + \sqrt{D})$
 $E_1 := \frac{(B - \sqrt{D_1}) \sin \beta_3 (\cos \alpha_2 - \sin \alpha_2 / \tan \beta_2) / \sin \alpha_2 + 2C}{(B + \sqrt{D_1}) \sin \beta_3 (\cos \alpha_2 - \sin \alpha_2 / \tan \beta_2) / \sin \alpha_2 + 2C}$

E_D : disc friction loss
 E_p : loss due to pumping at inactive arc of admission per unit mass flow rate (= N_p / G)
 G : flow rate through turbine
 ΔG : leakage flow rate due to partial admission
 H : blade height
 l : camber line length
 L : equivalent length of rotor channel
 N_p : pumping loss
 R : degree of reaction
 Re : Reynolds number (= Du/ν)
 s_t : tip clearance
 T : absolute temperature
 t_s : blade spacing
 t_e : blade trailing edge thickness projection of wheel
 u : wheel tangential velocity
 V_L : theoretical leakage velocity
 $V_R := c_2 / V_L - \xi \Delta L / H \sin \alpha_2$
 y : distance along nozzle arc from entering end
 α : absolute flow angle
 β : relative flow angle
 δ^* : boundary displacement thickness
 ϕ : flow coefficient
 ψ : load coefficient
 θ : boundary layer momentum thickness
 η_{it} : total to total efficiency
 η_{is} : total to static efficiency
 η_{tran} : coefficient of entering end and leaving end loss
 ϵ : degree of admission
 ζ : shock loss coefficient at rotor inlet
 ζ_p : profile loss coefficient
 ζ_e : end wall loss coefficient
 ζ_{cl} : tip clearance loss coefficient
 Δ : space between nozzle and rotor at pitch circle diameter
 Δ_L : leakage space between nozzle and rotor
 w : relative velocity

SUBSCRIPTS

1 : nozzle inlet
 2 : nozzle outlet and rotor inlet
 3 : rotor outlet
 N : nozzle
 R : rotor
 0 : stagnation

1. INTRODUCTION

With increasing gas pressure before a turbine stage, the nozzle admission area becomes smaller for the same power or mass rate of flow. A reduction of admission area may be achieved by decreasing the stator blade height and thus the aspect ratio of stator and rotor. It may also be accomplished by admitting the driving fluid to only a fraction of the nozzle annulus. The latter configuration is called partial admission. Both these ways of reducing the nozzle area result in a decrease in turbine efficiency. Even in a partial admission turbine there is a question of whether to use long blades and short admission arc for given mass rate of flow or vice versa.

Partial admission turbine is often used in the first stage of multistage turbines and more commonly in small auxiliary turbines.

This paper focuses on performance prediction of partial admission turbines on the basis of fluid dynamic studies of partial admission losses. The generalized loss coefficients for partial admission axial flow turbines are derived as a function of key geometrical parameters. It becomes feasible to find the particular geometry which maximizes efficiency for a particular set of operating conditions.

2. BREAK DOWN OF STAGE LOSSES

Before proceeding to deal with the losses in detail, it is convenient to consider first the nature of the losses in a stage. Profile loss, end wall loss, tip clearance loss and disc friction loss exist in partial admission turbines as well as in full admission turbines. Furthermore partial admission turbines have more loss sources than full admission turbines. The additional loss types are: (1) entering end loss occurring at beginning of the active arc of admission, (2) leaving end loss occurring at the end of the active arc of admission, (3) loss due to pumping by the blades in the inactive portion of arc, and (4) loss due to leakage of live gas between the rotor and stator. Fig.1 illustrates the positions where the above losses occur.

3. RELATIONS OF PARTIAL ADMISSION LOSSES

New correlations for the losses due to partial admission are proposed here.

(a) ENTERING END LOSS and LEAVING END LOSS

When a blade channel filled with stagnant fluid begins to enter the admission sector, the live fluid from the nozzle entering this channel has to eject the stagnant fluid. This process of "scavenging" the blade channel entering the admission sector may continue for some time before a steady flow is established. Due to the presence of this "transitional zone" of unsteady flow, the nozzle jet entering the rotor blades in this zone

suffers momentum loss leading to work loss on the blades. On the other side, when a blade channel begins to leave the admission sector, the flow in the blade channel changes to a pumping flow in the inactive portion of arc. The aerodynamic loss also occurs in this transient zone.

Fig.2 shows the non-dimensional relations of the flow velocities and the flow angles at the transient zones which are deduced from the nonsteady flow analysis and the experiment using a single stage axial flow turbine carried out by the authors [1]. Here the equations in Fig.2 can be expressed as follows:

$$\frac{C_{xp}}{C_x} = \frac{\frac{\sin \beta_3}{\sin \alpha_2} (\cos \alpha_2 - \frac{\sin \alpha_2}{\tan \beta_2}) \{E(B + \sqrt{D}) e^{-\sqrt{D} \frac{y}{L}} - B + \sqrt{D}\}}{2C \{1 - E e^{-\sqrt{D} \frac{y}{L}}\}} \quad (0 \leq y \leq y_A) \quad (1)$$

$$C_{xp}/C_x = 1 \quad (y_A \leq y \leq 2y_A + y_B) \quad (2)$$

$$C_{xp}/C_x = 1 - 0.2(y - 2y_A - y_B)/y_c \quad (2y_A + y_B \leq y \leq 2y_A + y_B + y_c) \quad (3)$$

$$\frac{C_{xp}}{C_x} = \frac{\frac{\sin \beta_3}{\sin \alpha_2} (\cos \alpha_2 - \frac{\sin \alpha_2}{\tan \beta_2}) \{E_1(B - \sqrt{D_1}) e^{-\sqrt{D_1} \frac{y - E\pi D_m}{L}} - B - \sqrt{D_1}\}}{2C \{1 - E_1 e^{-\sqrt{D_1} \frac{y - E\pi D_m}{L}}\}} \quad (2y_A + y_B + y_c \leq y \leq 2y_A + y_B + y_c + y_D) \quad (4)$$

$$\alpha_{1p} = \alpha_1 \quad (0 \leq y \leq 2y_A + y_B + y_c + y_D) \quad (5)$$

$$\alpha_{2p} = \alpha_2/2 \quad (0 \leq y \leq y_A) \quad (6)$$

$$\alpha_{2p} = \alpha_2 y/2y_A \quad (y_A \leq y \leq 2y_A) \quad (7)$$

$$\alpha_{2p} = \alpha_2 \quad (2y_A \leq y \leq 2y_A + y_B) \quad (8)$$

$$\alpha_{2p} = \cot^{-1} \left(\frac{u}{C_{xp}} + \cot \beta_2 \right) \quad (2y_A + y_B \leq y \leq 2y_A + y_B + y_c + y_D) \quad (9)$$

By use of the above relations, the ratio of specific work (work per unit flow rate) developed by the turbine cascade working under partial admission to under full admission can be derived

$$\eta_{tran} = \frac{\int_0^{2y_A + y_B + y_c + y_D} \rho C_{xp}^2 (\cot \alpha_{2p} - \cot \alpha_{3p}) dy}{\int_0^{E\pi D_m} \rho C_{xp} dy} \quad (10)$$

which indicates the entering end loss and leaving end loss. The calculated result of equation (10) is shown in Fig.3. Ohlsson's theory [2] also has been added to this figure. Since Ohlsson's theory is developed under the assumptions: (1) frictionless and incompressible flow, (2) infinite number of blades in the rotor and one dimensional flow through the rotor blades, Ohlsson's theory underestimates the losses than the result of equation (10) at any value of u/c_2 . At greater value of u/c_2 , the difference between equation (10) and Ohlsson's theory is remarkable.

(b) BLADE PUMPING LOSS

A recirculating flow which enters at the base of the blade and leave at the tip is induced by the blades at the inactive portion of the arc as shown in Fig.4. To induce this recirculating flow leads to power loss. This type of loss is known as blade pumping loss. The blade pumping loss was already investigated in [3],[4],[5].

In actual machines as in any case where working-fluid flow through a turbine occurs, the interaction between the pumping flow and the working-fluid flow at the clearance between the nozzle and the rotor on the pumping loss has to be considered. But it is very difficult to determine the effect of this interaction in actual machines. Therefore the experiments to simulate this effect are carried out in the present paper.

A general layout of the test rig is shown in Fig.5. The thin plate along the nozzle cuts off the pumping flow between the nozzle and the rotor. Fig.6 shows the experimental results of axial velocities and flow angles around the plate at the rotor outlet. As shown in Fig.6, since the pumping flow is affected by cutting the flow between the nozzle and rotor, it can be considered that the value of pumping loss depends on the interaction effect of working fluid flow. Fig.7 shows the experimental results of coefficient of the pumping loss defined as

$$C = \frac{N_p}{\pi D_m H \rho u^3 / 2} \quad (11)$$

The value of C without the plate almost coincides with a line which is calculated result of the empirical equation proposed by Suter and Traupel [3]. The value of C increases with increasing the number of the plates along the nozzle which is arranged as shown in Fig.7. The number of plates simulates the inactive arc of admission Θ (= length of inactive sector/length of whole periphery of the wheel), that is one plate simulates $\Theta \doteq 1$ (active fluid flow exist but almost region is inactive arc), two plates simulate two of $\Theta = 1/2$, three plates simulate three of $\Theta = 1/3$, four plates simulate four of $\Theta = 1/4$, respectively.

Then we rewrite the equation (11) as

$$C = C_0 \lambda = \frac{N_p}{\pi D_m H \rho u^3 / 2} \quad (12)$$

where C_0 denotes the loss coefficient without considering the interaction effect of working fluid flow being an empirical function in [3] and λ denotes the correction factor due to the interaction effect of working fluid flow whose values are shown in Fig.8. As shown in Fig.8, the value of λ increases with increasing the ratio of axial distance to the blade height but does not depend on the blade configuration. Then the simple correlation of are proposed here:

$$\begin{aligned} \lambda &= 1 + 0.15\Theta & \text{for } \Delta/H &= 0.47 \\ \lambda &= 1 + 0.1\Theta & \text{for } \Delta/H &= 0.32 \\ \lambda &= 1 + 0.03\Theta & \text{for } \Delta/H &= 0.16 \end{aligned} \quad (13)$$

(c) LEAKAGE LOSS

Leakage through the clearance space between the stator and the rotor from the active regions to inactive regions takes place in partial admission turbines. This leakage can be divided into two parts: (1) circumferentially between stator and rotor blades, (2) radially between stator and rotor rim. As the circumferential leakage flow essentially interacts with the working fluid flow at the entering end and the leaving end, it is difficult to estimate the loss due to this leakage separately. In this paper the circumferential leakage loss is ignored because the entering end loss and the leaving end loss are treated semiempirically based on the measured values of flow velocities and flow angles which contain the effect of the interaction between the leakage and the working flow. Thus we consider only the radial leakage between stator and rotor rim. Since the radial leakage flow can be considered to do little or no work, the expression for leakage loss becomes

$$[\text{debits of work due to leakage}] = \Delta G \times [\text{work done in blading}].$$

The leakage fraction $\Delta G/G$ can be expressed as

$$\frac{\Delta G}{G} = \frac{\xi \Delta_L V_L}{C_2 H \sin \alpha_2} \quad (14)$$

where V_L denotes the theoretical leakage velocity which is defined as

$$V_L = C_2 \sqrt{\frac{2 R \sin^2 \alpha_2 (\cot \alpha_2 - \cot \alpha_3)}{\phi} + 1} \quad (15)$$

and ξ denotes the leakage flow coefficient which is given as

$$\begin{aligned} \xi &= 1 - \frac{1}{\pi} \frac{H \sin \alpha_2}{\Delta_L} \left\{ \log_e \left| \frac{1 - C_2/V_L}{1 + C_2/V_L} \right| + \left(\frac{C_2}{V_L} \right)^2 \log_e \left| \frac{1 - V_L/C_2}{1 + V_L/C_2} \right| \right. \\ &\quad \left. - \log_e \left| \frac{1 - V_R}{1 + V_R} \right| - V_R^2 \log \left| \frac{1 - 1/V_R}{1 + 1/V_R} \right| \right\} \end{aligned} \quad (16)$$

under the conditions of $\delta^* \sin \alpha_2 / \Delta_L < 1.5$ and $\delta \sin \alpha_1 / \Delta_L < 0.2$. Equation (16) was derived theoretically and was confirmed by the experiments as already reported by the authors[1].

4. EFFICIENCY

The definition of the stage efficiency depends on the application. In a multi-stage machine the efficiency is best defined as "total to total" efficiency:

$$\eta_{it} = \frac{\text{Actual work output}}{\text{Maximum adiabatic work output in operating to the same back pressure}} \quad (17)$$

If exhaust kinetic energy is not used (e.g. as in a single stage turbine without an exhaust diffuser) then the efficiency should be defined as a "total to static efficiency":

$$\eta_{is} = \frac{\text{Actual work output}}{\text{Isentropic work obtained in expansion to the exhaust back pressure at zero leaving velocity}} \quad (18)$$

If profile loss, end wall loss and tip clearance loss are expressed in the enthalpy loss coefficient and disc friction loss, blade pumping loss and leakage loss are expressed as the power loss per unit mass flow rate of the working fluid, the expression of the efficiencies can be given by

$$\eta_{it} = \left\{ (1 - \Delta G/G_T) \eta_{tran} \phi (\cot \alpha_2 - \cot \alpha_3) - (\bar{E}_D + \bar{E}_P)/U^2 \right\} / \left\{ \phi (\cot \alpha_2 - \cot \alpha_3) + \left(\frac{\zeta_{PN} + \zeta_{EN}}{1 - \zeta_{PN} - \zeta_{EN}} \right) \frac{\phi^2}{2 \sin^2 \alpha_2} + \left(\frac{\zeta_{PR} + \zeta_{ER} + \zeta_{CL}}{1 - \zeta_{PR} - \zeta_{ER} - \zeta_{CL}} \right) \frac{\phi^2}{2 \sin^2 \beta_3} \right\} \quad (19)$$

$$\eta_{is} = \left\{ (1 - \Delta G/G_T) \eta_{tran} \phi (\cot \alpha_2 - \cot \alpha_3) - (\bar{E}_D + \bar{E}_P)/U^2 \right\} / \left\{ \phi (\cot \alpha_2 - \cot \alpha_3) + \left(\frac{\zeta_{PN} + \zeta_{EN}}{1 - \zeta_{PN} - \zeta_{EN}} \right) \frac{\phi^2}{2 \sin^2 \alpha_2} + \left(\frac{\zeta_{PR} + \zeta_{ER} + \zeta_{CL}}{1 - \zeta_{PR} - \zeta_{ER} - \zeta_{CL}} \right) \frac{\phi^2}{2 \sin^2 \beta_3} + \frac{\phi^2}{2 \sin^2 \alpha_3} \right\} \quad (20)$$

The equations (19) and (20) are derived on the assumptions of $\phi_2 = \phi_3 = \phi$ and $T_{3s} = T_2$. These assumptions are valid so long as the pressure ratio is low.

No new correlations for the loss coefficient ζ_{PN} , ζ_{PR} , ζ_{EN} , ζ_{ER} , ζ_{CL} , \bar{E}_D in equations (19) and (20) are proposed in this paper. These values are calculated by the relations proposed by Balje [6] without alternation.

5. PERFORMANCE MAPS

A theoretical method of performance prediction has the advantage that it gives the designer a method by which the relative performance merits of varying arrangements can be assessed in the early design phase. For preliminary design studies it is useful to construct generalized performance map which predict the stage efficiency changes that are implied by the variation of certain basic aerodynamic parameters. Three such maps are presented in Fig. 9, 10 and 11. Fig. 9 shows the calculated total to total efficiency for zero reaction turbines working under full and partial admission. In Fig. 9 the solid lines, the dotted lines and the dot-dash lines indicate $\xi = 1.0$ (full admission), $\xi = 0.5$ and $\xi = 0.25$, respectively. Fig. 9 shows the maximum efficiencies decrease and the value of ϕ and ψ which give the maximum efficiency increase as the degree of admission ξ decreases. Fig. 10 is a performance map of the 50% reaction turbines. From Fig. 9 and Fig. 10 the maximum efficiencies can be read as follows:

turbine \ degree of admission ξ	1.0	0.5	0.25
impulse	92 %	86 %	81 %
50% reaction	95 %	86 %	81 %

The 50% reaction turbines have higher maximum efficiency than the impulse turbines under full admission condition, but have almost same value of maximum efficiency under partial admission condition of $\xi = 0.5$ and $\xi = 0.25$ because of the existence of the leakage loss due to partial admission. If the axial distance is selected larger value than the given value in Fig. 10, the leakage loss increases, consequently the maximum efficiency of the 50% reaction turbine indicates lower than of impulse turbine under partial admission. Therefore we design the high reaction partial admission turbines, the above fact have to be considered. Fig. 11 shows a performance map of single stage turbines based on total to static efficiency. Comparison of Fig. 9 and Fig. 11 indicates that the value of η_{is} is less than the value of η_{it} , because the loss in exhaust kinetic energy has dominant effect on η_{is} .

6. PARTIAL ADMISSION vs. LOW ASPECT RATIO

In general if we design a small turbine, we have to select the optimum combination of degree of admission ξ and blade height (thus aspect ratio) which gives highest efficiency for given nozzle outlet area. To illustrate the design guidance of small turbines, the calculated result of η_{is} at $h/c = 0.25$ and $\xi = 1.0$, $h/c = 0.5$ and $\xi = 0.5$ and $h/c = 1.0$ and $\xi = 0.25$ which have the equal nozzle outlet area is shown in Fig. 12. As shown in Fig. 12 the maximum efficiency of the full admission turbine with low aspect ratio $h/c = 0.25$ is lower than that of partial admission turbine, because end wall loss is larger than partial admission losses. In this case, the partial admission turbine of $\xi = 0.5$ or $\xi = 0.25$ has to be selected.

As dimensionless parameters without ξ and h/c hold constant in Fig. 12, in practice this is generally insufficient. Because the optimum value of other dimensionless parameters change with the value of ξ and h/c . It is therefore necessary to determine the optimum combination of all parameters at given design specification or constraints in practical design problems.

ACKNOWLEDGMENT

Acknowledgment is due to Prof. M. Sakamoto for valuable discussion.

REFERENCES

- [1] K.Korematsu and N.Hirayama, "Fundamental Study on Compressible Transient Flow and Leakage in Partially Admitted Axial and Radial Flow Turbines" Proceedings of The Second International JSME Symposium Fluid Machinery and Fluidics, Vol.2 Sep. 1972 pp.191-201, and "Study on the losses in partial admission turbines", Transaction of JSME, Vol.41, No.341, 1975, pp.240-257 (Japanese)
- [2] G.O.Ohlsson, "Partial Admission Turbines" Journal of the Aerospace Sciences, Vol.29, No.4, 1962, pp1017-1023
- [3] P.Suter and Traupel, "Untersuchungen über den Ventilations-Verlust von Turbinrädern" Mitteilungen aus dem Institut für Thermische Turbomachines an der Eidgenössischen Technischen Hochschule in Zürich, Nr.4, 1959
- [4] R.W.Mann and C.H.Marston, "Friction drag on bladed disks in housings as a function of Reynold number, axial and radial clearance, blade aspect ratio and solidity" Transaction of ASME-D, 1961, pp.719-723
- [5] S.M.Yahya and M.D.C.Doyle, "Aerodynamic losses in partial admission turbines" International Journal of Mechanical Science Vol.11, 1969, pp.417-431
- [6] O.E.Balje and R.L.Binsly, "Axial Turbine Performance Evaluation part A--loss geometry relationships" Transaction of ASME-D, 1968, pp.341-348

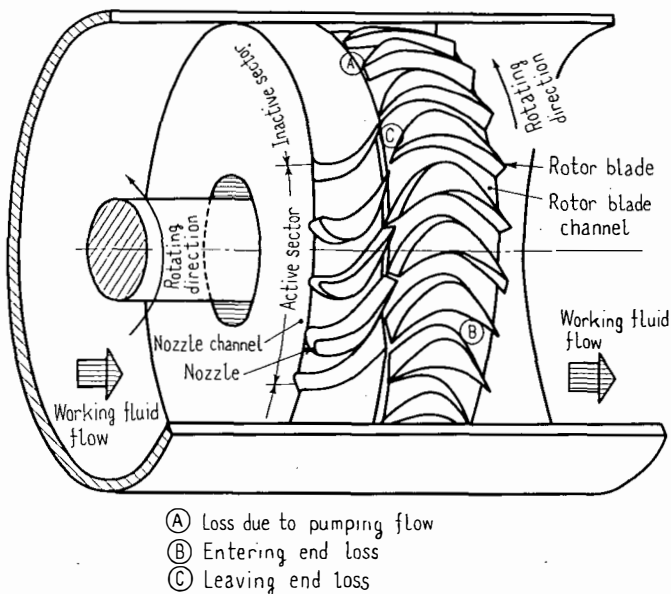


Fig. 1 Losses due to partial admission

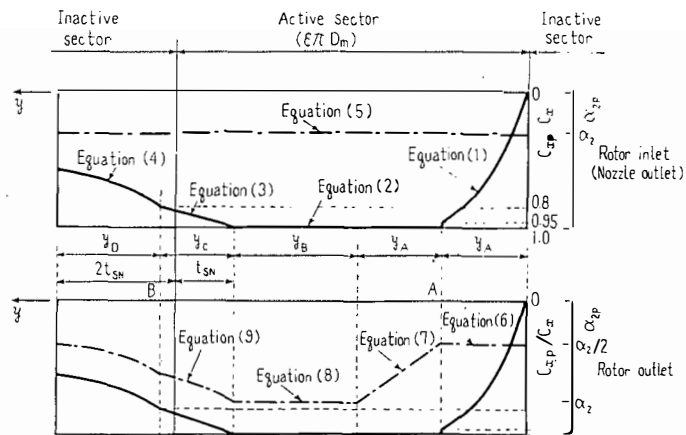


Fig. 2 Axial velocities and flow angles at rotor inlet and outlet in partial admission

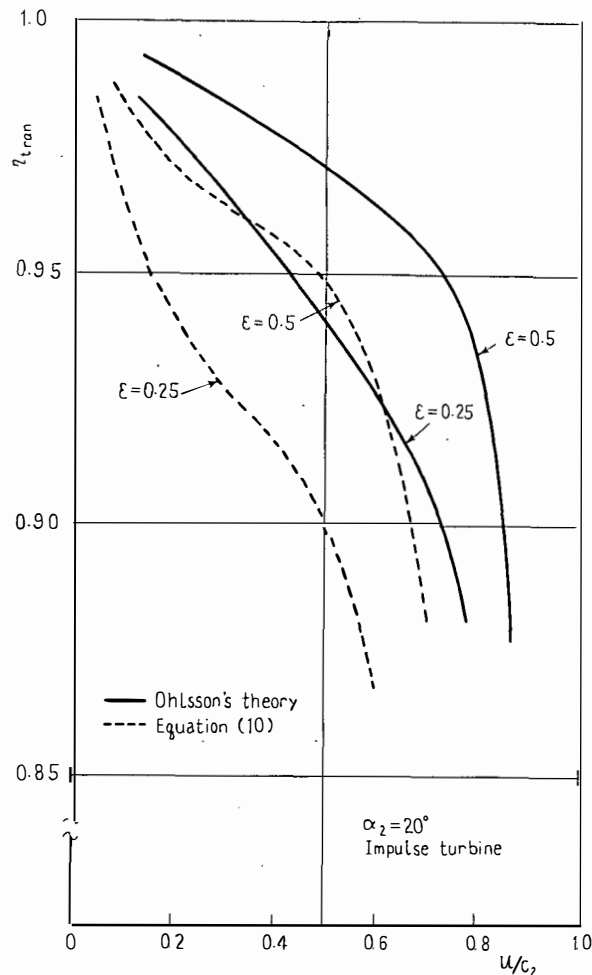


Fig. 3 Entering end loss and leaving end loss

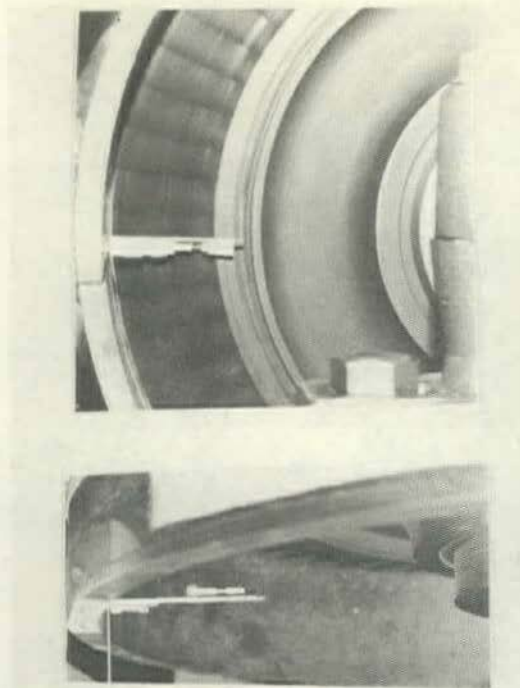


Fig. 4 Recirculating flow due to blade pumping

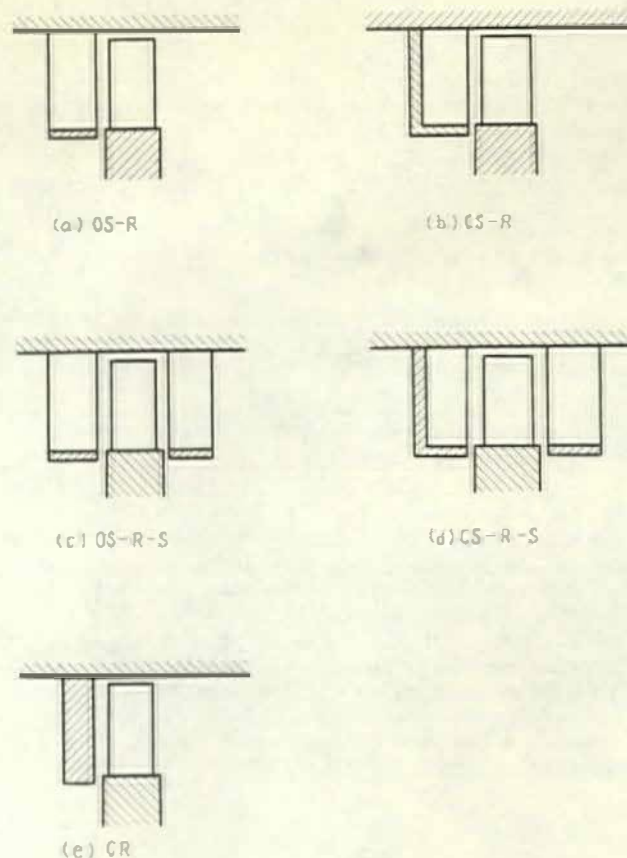


Fig. 5 (3) blade configuration

Fig. 5 Schematic drawing of test equipment

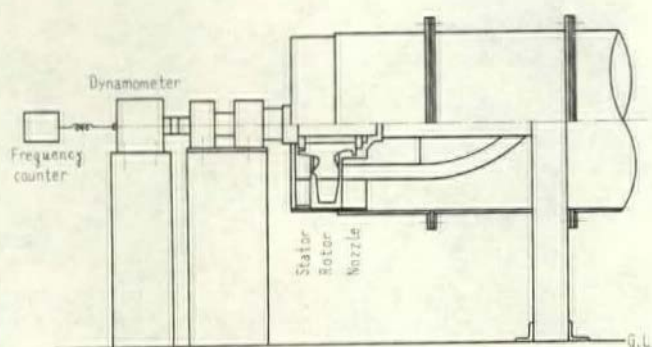


Fig. 5 (1) Test rig

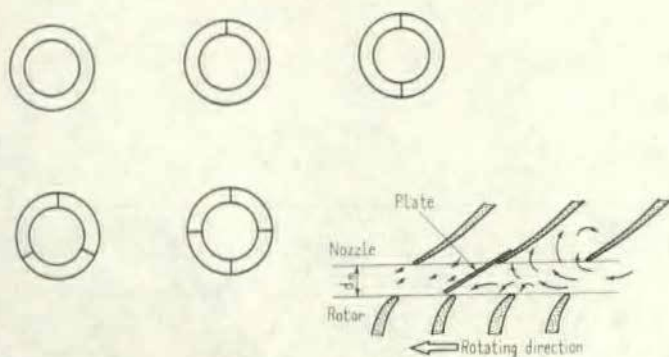


Fig. 5 (2) Arrangement of plates

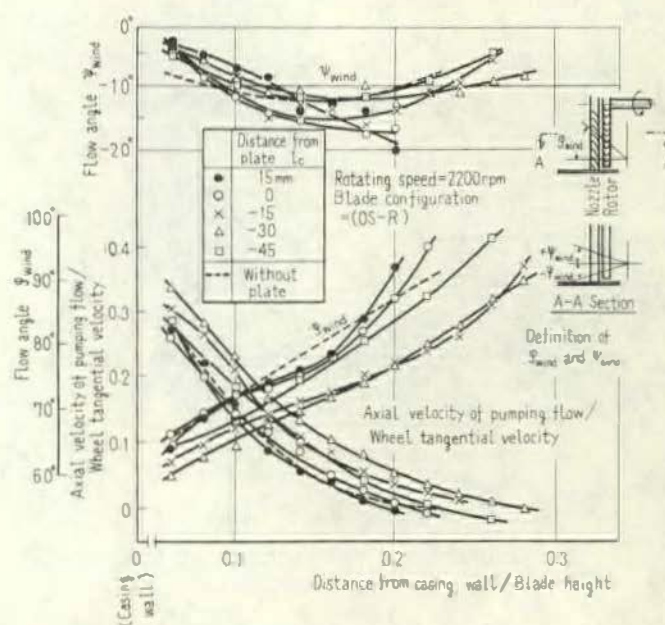


Fig. 6 Pumping flow near casing wall

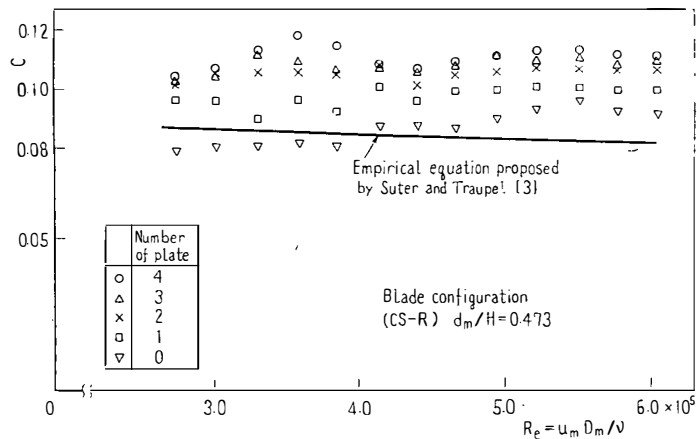


Fig. 7 Coefficient of pumping loss

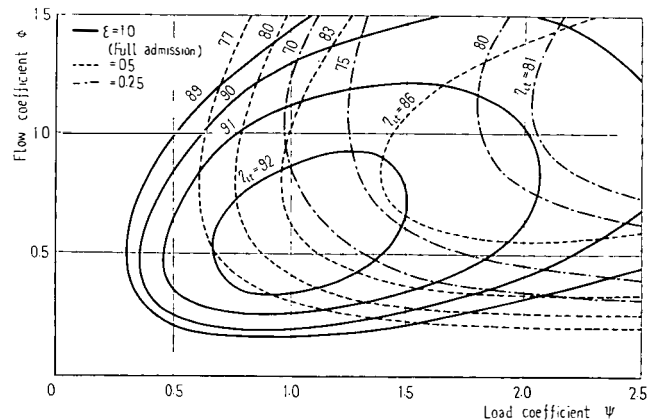


Fig. 9 Performance map based on it (impulse turbine)
 $(R=0, c_R/D_m=0.05, t_e/t_s=0.02, /D_m=0.02, (c/H)_R=0.5, /H_R=0.05, (c/H)_N=0.5, st/H_R=0.01, \beta_1=90 \text{ deg}, w_3c/ = 2 \times 10^5)$

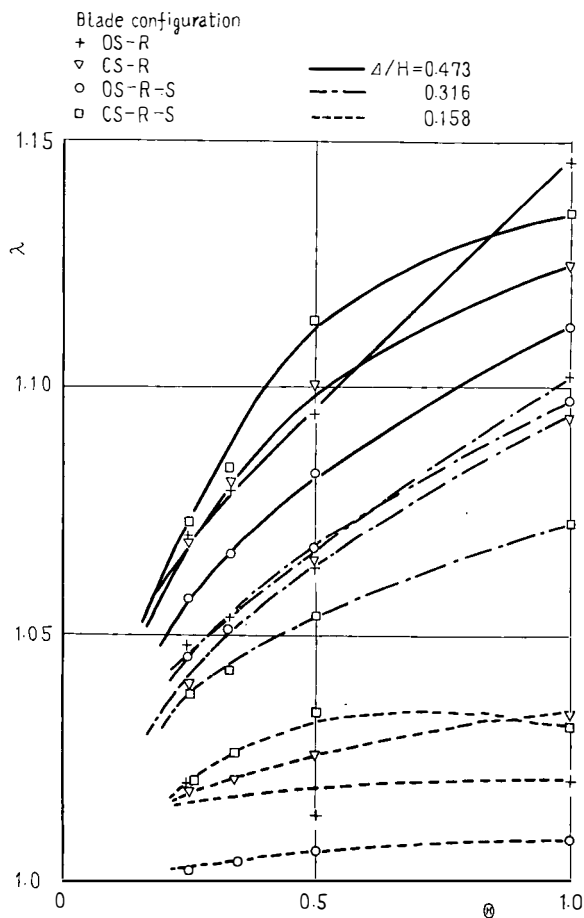


Fig. 8 Correction factor due to the interaction effect of working-fluid flow

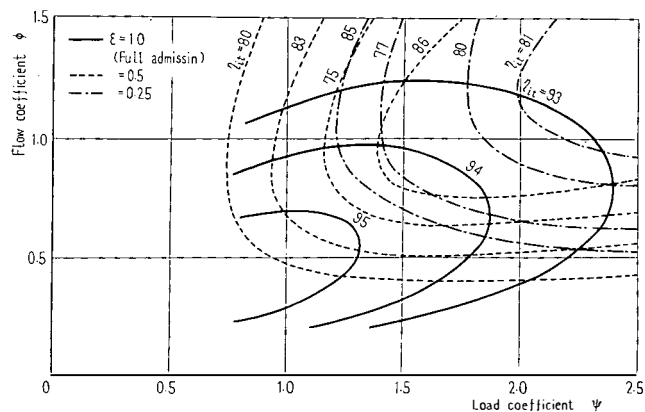


Fig. 10 Performance map based on it (50 percent reaction turbine)
 $(R=0.5, c_R/D_m=0.05, t_e/t_s=0.02, /D_m=0.02, (c/H)_R=0.5, \beta_1/H_R=0.05, (c/H)_N=0.5, st/H_R=0.01, \beta_1=90 \text{ deg}, w_3c/ = 2 \times 10^5)$

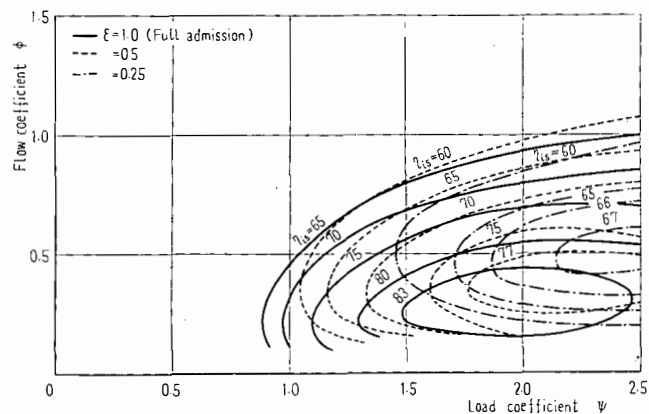


Fig. 11 Performance map based on i_s (impulse turbine)
 $(R=0, c_R/D_m=0.05, t_e/t_s=0.02, l/D_m=0.02, (c/H)_R=0.5, L/H_R=0.05, (c/H)_N=0.5, s_t/H_R=0.01, \beta_1=90^\circ, w_3c/\omega=2 \times 10^5)$

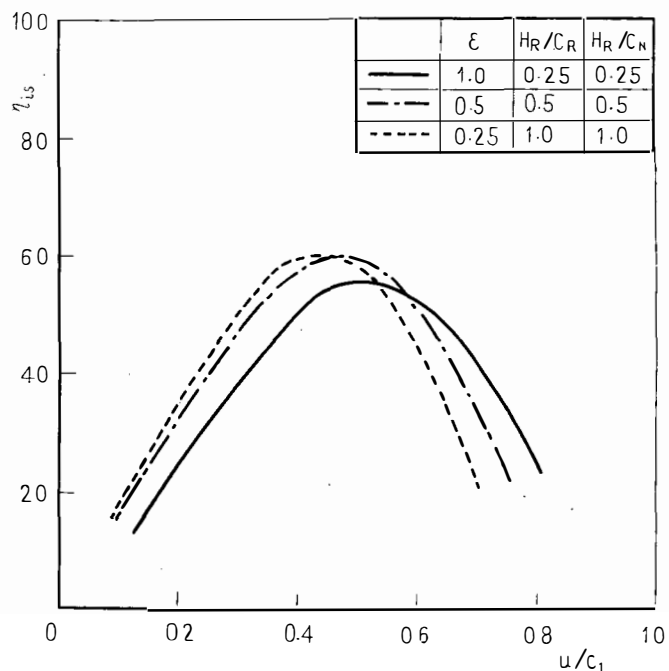


Fig. 12 Partial admission versus low aspect ratio
 $(R=0, \beta_1=90^\circ, \beta_2=20^\circ, H/D_m=0.1, s_t/H=0.15, l/D_m=0.02, t_e/t_s=0.02, l/H=0.1, w_3c/\omega=2 \times 10^5)$